Sci. Rep. RITU A41 (1995) pp. 1-8
No. 1, March 1995

Molecular Dynamics Study for Structure and Dynamics of Amorphous and Liquid $Zr_{67}Ni_{33}$ Alloys*

Tomoyasu AIHARA, Jr., Yoshiyuki KAWAZOE and Tsuyoshi MASUMOTO
Institute for Materials Research, Tohoku University, Sendai 980-77
(Received January 31, 1995)

Molecular dynamics simulations have been performed for $Zr_{67}Ni_{33}$ amorphous and liquid alloys with a pair functional potential. The temperature dependence of the structure is studied. The temperature derivative of the full width at half maximum of the pair distribution function changes at the glass transition temperature. The non-collective single particle motion is analyzed by the velocity autocorrelation function (VACF) and its power spectra. The mutual and self diffusion coefficients are calculated. The collective dynamics is analyzed by the intermediate scattering function. It clearly reveals two relaxation processes below the melting point. For the equilibrium liquid state, the relaxation is detected as one process. The size effect of MD system is examined for the structure. Most of the important physical properties except for long range correlation is enough well determined by a small system. The accuracy of the transport coefficient derived from Green-Kubo formula is discussed.

KEYWORDS: molecular dynamics (MD), glass transition, amorphous, pair distribution function, Green-Kubo formula, intermediate scattering function

1. Introduction

Amorphous alloys are experimentally produced mainly by rapid quenching (RQ) from the melt. If a liquid alloy is cooled at a rate of the order of $10^6 Ks^{-1}$, it enters the supercooled liquid regime and its viscosity increases tremendously. Finally, the system reaches a state of frozen random structure, i.e. amorphous state. The glass transition of the amorphous alloys has mainly been detected by specific heat measurement. In most of these alloys, however, it is difficult to measure other properties of amorphous and liquid phases at high temperature, because of the crystallization. In the attempt to control the properties of amorphous alloys, it is important to understand the atomistic behavior of the glass transition.

To investigate the atomistic properties of the matter at the solid and liquid states molecular dynamics (MD) simulation has intensively been performed. [1] The substance of MD simulation is a numerical experiment to solve the N-body problem of Newtonian mechanics. [2] By MD simulation, we can treat the material at atomic level. As the observation time in MD simulation at present is an order of picoseconds, the amorphous and supercooled liquid materials are treated without crystallization. MD studies for the glass transition have been performed for relatively simple materials, for example, the Lennard-Jones system to research common behavior of simple systems. [3, 4, 5] Various matters take the amorphous state and their properties strongly depend on their chemical bonding nature. We have performed MD simulation for $Zr_{67}Ni_{33}$ alloy in the equilibrium liquid, the supercooled liquid and the amorphous state. [6, 7, 8, 9, 10] To examine the properties of the metallic bonding system, we use the pair functional potential. We have already reported on the thermodynamical value [6], the microscopic energy fluctuation [7], statistical structure [6] and the phonon dispersion relation [8, 9]. We found the simulated glass transition temperature of this system to be 640K [6], which is close to the calorimetrically determined experimental value of 652K.[11] The enthalpy change of crystallization [12], X-ray weighted structure factor of amorphous state [13] and the vibrational energy distribution [14] are also reproduced well by our MD simulations. [6, 8]

In this paper, we perform on MD simulation for $Zr_{67}Ni_{33}$ alloy at varoius temperatures from the equilibrium liquid to the amorphous state. We study the change of the physical properties through the glass transition. Fine distinction of static structure is analyzed by pair distribution function. Time dependent structure is calculated as intermediate scattering function. Vibrational dynamics is examined by velocity correlation function and its spectrum. Moreover, we analyze size effect in the MD on the structure. The origin of the structural change through the glass transition and the MD size effect for the macroscopic dynamical property calculation are discussed.

2. Method of Computation

The present MD simulations are carried out for $Zr_{67}Ni_{33}$ alloy with periodic boundary conditions. The total number of atoms in the simulated system is 960 or 7680. The overall concentration is Zr:Ni=2:1. We use the Nosé constant-temperature (NVT) method [15] with a modification in which the volume is expressed as a function of the object temperature. The density of the amorphous structure is 7.06 Mgm^{-3} at 298K, which agrees with the experimental value. [16] It is assumed that the system has the constant thermal expansion coefficient of $2.659 \times 10^{-5} K^{-1}$. This approximation is reasonable because the glass transition is the transformation from liquid to solid states without discontinuous change in volume. The calculation starts by constructing a C16 tetragonal crystal structure (4x4x5 lattice cells parallel to the periodic box). The system is first heated well above the melting temperature (T_m=1393K), [17] i.e. up to 2000K, to obtain a homogeneous equilibrium liquid state. The system is then quenched quasi-continuously to various object temperatures with a quench rate of $2 \times 10^{14} K^{-1}$ by scaling the velocities. After subsequent isothermal annealing at the object temperature, statistical analyses of the time series data are performed. The equations

* IMR, Report No. 1990

of motion are solved using the fifth-order predictor corrector algorithm of Gear with a time step of 1 fs. We use the MPM (Massobrio, Pontikis and Martin) pair functional potential. [18] The potential energy of the system is written as

$$E_{pot}=\sum_{\alpha=1}^{m}\sum_{i_\alpha}^{N_\alpha}\left[\sum_{\beta=1}^{m}\sum_{j_\beta(\neq i_\alpha)}^{N_\beta}A_{\alpha\beta}\exp\left[-p_{\alpha\beta}\left(\frac{r_{i_\alpha j_\beta}}{d_{\alpha\beta}}-1\right)\right]-\left\{\sum_{\beta=1}^{m}\sum_{j_\beta(\neq i_\alpha)}^{N_\beta}\xi_{\alpha\beta}^{2}\exp\left[-2\,q_{\alpha\beta}\left(\frac{r_{i_\alpha j_\beta}}{d_{\alpha\beta}}-1\right)\right]\right\}^{1/2}\right], \quad (1)$$

where $r_{i_\alpha j_\beta}$ is the distance between i_α and j_β atoms. The latter functional term represents the many-body interactions in metal. They fitted the potential to reproduce the thermodynamical and elastic properties of the crystal. [18] We have studied MD simulations on amorphous and liquid $Zr_{67}Ni_{33}$ alloys by this potential. [6, 7, 8, 9, 10] Physical properties are reproduced well by our MD simulations. [6, 8] This reproducibility means the appropriateness to apply the MPM potential to the MD simulation in liquid and amorphous phases.

In MD simulation for isotropic substance, the real space structural information is obtained as pair distribution function $g(r)$ at first as [19]

$$g(r)=\frac{1}{4\pi r^2\rho_0}\frac{1}{N}\left\langle\sum_{i}^{N}\sum_{j(\neq i)}^{N}\delta\left[r-r_{ij}\right]\right\rangle, \quad (2)$$

where ρ_0 is the number density, N the number of the atoms, r_{ij} the distance between i and j atom and $\langle\cdots\rangle$ the time average. The structure factor is calculated as Fourier transformation of the pair distribution function,

$$S(Q)=1+\int_0^\infty 4\pi r\rho_0\left[g(r)-1\right]\frac{\sin(Qr)}{Q}dr. \quad (3)$$

The pair distribution function for the partial part is defined as Faber-Ziman (FZ) form. Moreover, the Batia-Thornton (BT) type pair distribution functions are calculated from the FZ form. [20] The particle number term $g_{NN}(r)$, the concentration term $g_{CC}(r)$, and their cross term $g_{NC}(r)$, are defined as follows,

$$g_{NN}(r)=c_A^2 g_{AA}(r)+c_B^2 g_{BB}(r)+2c_A c_B g_{AB}(r), \quad (4)$$

$$g_{NC}(r)=c_A c_B\left[c_A g_{AA}(r)-c_B g_{BB}(r)+\left(c_B-c_A\right)g_{AB}(r)\right], \quad (5)$$

$$g_{CC}(r)=c_A c_B\left[1+c_A c_B\left\{g_{AA}(r)+g_{BB}(r)-2g_{AB}(r)\right\}\right], \quad (6)$$

where c_A and c_B is the concentrations of the A and B atoms.

The structure independent dynamics are analyzed by the velocity autocorrelation function (VACF), [19] which is defined by

$$\psi(t)=\frac{\sum_{i=1}^{N}\left\langle v_i(0)\cdot v_i(t)\right\rangle}{\sum_{i=1}^{N}\left\langle v_i(0)\cdot v_i(0)\right\rangle}, \quad (7)$$

where $v_i(t)$ is the velocity of the i atom at time t. The power spectrum at angular frequency ω is calculated as the Fourier transform of the VACF,

$$Z(\omega)=\frac{2}{\pi}\int_0^\infty\frac{1}{N}\sum_{i=1}^{N}\left\langle v_i(0)\cdot v_i(t)\right\rangle\cos(\omega t)dt. \quad (8)$$

For a binary mixture of components A and B, the Green-Kubo expression for the mutual diffusion coefficient is used, [21]

$$D_{AB}=\frac{1}{3N}\left(\frac{\partial^2(G/Nk_BT)}{\partial c_A^2}\right)\int_0^\infty\left\langle j_{AB}(t)\cdot j_{AB}(0)\right\rangle dt. \quad (9)$$

Here G is the mixture Gibbs free energy and $j_{AB}(t)$ is defined as

$$j_{AB}(t)=c_B\sum_{i_A=1}^{N_A}v_{i_A}(t)-c_A\sum_{i_B=1}^{N_B}v_{i_B}(t). \quad (10)$$

If we approximate the mixture as an ideal solution, the derivative in equation (9) becomes

$$\frac{\partial^2(G/Nk_BT)}{\partial c_A^2}=\frac{1}{c_A c_B}. \quad (11)$$

The structure dependent dynamics in real space are estimated from the van Hove correlation function, [19]

$$G(r,t)=\frac{1}{N}\sum_{i=1}^{N}\sum_{j=1}^{N}\left\langle\delta\left(\left|r_i(t)-r_j(0)\right|-r\right)\right\rangle, \quad (12)$$

where $r_i(t)$ denotes the position of the atom i at time t. The intermediate scattering function $F(Q,t)$ shows the time course of the density correlation in reciprocal space. It is calculated from the Fourier transformation of the van Hove correlation function as,

$$F(Q,t)=\int_0^{r_c}G(r,t)\frac{\sin(Qr)}{Qr}dr. \quad (13)$$

This is equivalent to the coherent part. The incoherent part is calculated from Fourier transformation of the self part of the van Hove correlation function which is defined as

$$G^s(r,t)=\frac{1}{N}\sum_{i=1}^{N}\left\langle\delta\left(\left|r_i(t)-r_i(0)\right|-r\right)\right\rangle. \quad (14)$$

3. Results

3.1. Structure

We first examine the system size effect in the present MD simulation. Because the structure is the fundamental microscopic information of amorphous and liquid materials, we compare the structures of equilibrium liquid for 960 and 7680 atom systems. The MD cell length of the latter is double of the former. Figure 1 shows the particle number term of the pair distribution function at 2000 K. Although it is possible for the 7680 atom system to estimate better the long range correlation, the basic profile of the distribution function is almost equivalent for both systems. Figure 2 shows the structure factor at 2000 K. The fluctuation of the structure factor at low wave number is caused by the cut off error of the Fourier transformation for the 960 atom system. This error also causes the first peak height difference between 960 and 7680 atom system. The basic profile, the shape and position of first and high wave number peak for the 960 atom system are equivalent to those for the 7680 atom systems. Since the computation cost on MD simulation is proportional to the square of the atom number of the system, and the 960 atom system provides the same results as the 7680 atom system except for long range correlation, we perform MD simulation mainly for the 960 atom system.

The BT type pair distribution function is calculated as a function of temperature. Figure 3 shows the particle number term N-N, the concentration term C-C and their cross term N-C of the pair distribution function. The concentration term functions are normalized by the product of the concentration. The temperature dependence of the pair correlation function reveals an essentially continuous change from the liquid to the amorphous states. The feature changes sharper with decreasing temperature. The first peaks for the particle number term split under melting temperature. These sub-peaks are related to the pair correlation in FZ form. In the equilibrium liquid state, splitting of the first peak is not observed because of the heavy thermal fluctuation. The splitting of the second peak in the particle number term is not clear even at very low temperature. The concentration term of the normalized pair distribution function is saturated to 1 over the second neighbor atom distance. This means that the long-range concentration fluctuation is small at all temperatures. In an equilibrium liquid state, the concentration fluctuation exists only for short distance. The cross term does not show strong temperature dependence.

For the analysis of detailed distinction of pair distribution function, we estimate the full width at half maximum (FWHM) of the first peak of the FZ type pair distribution function as shown in Fig. 4. The FWHM increases with temperature. This increment is mainly caused by the thermal vibration. The FWHM for the Ni-Ni correlation is smaller than that for Zr-Zr and Zr-Ni correlation by about 30%. This indicates that the fluctuation of the interatomic distance of Ni-Ni pair is smaller than that of Zr-Ni and Zr-Zr pairs. The slopes of the FWHM change at the thermally determined glass transition temperature of 640 K. The increments are 12% for Zr-Zr, 31% for Zr-Ni and 48% for Ni-Ni correlations. The slight change of the structure through the glass transition temperature is also detected by Wendt-Abraham parameter, [22] the ratio of the first minimum and the first maximum of the pair distribution function. [6]

3.2. Dynamics

The dynamics of atom motion is treated by two different view points. One is the collective motion, and the other is the non-collective single particle motion. We first analyze single particle motion. Figure 5 shows the VACFs for Zr atom. A strong backscattering near 0.1ps and the subsequent oscillations are observed in the amorphous state. At 1400K, in the equilibrium liquid state, backscattering is weak and oscillation converges fast. This behavior is typical of dense fluid. Over the glass transition temperature, the behavior of

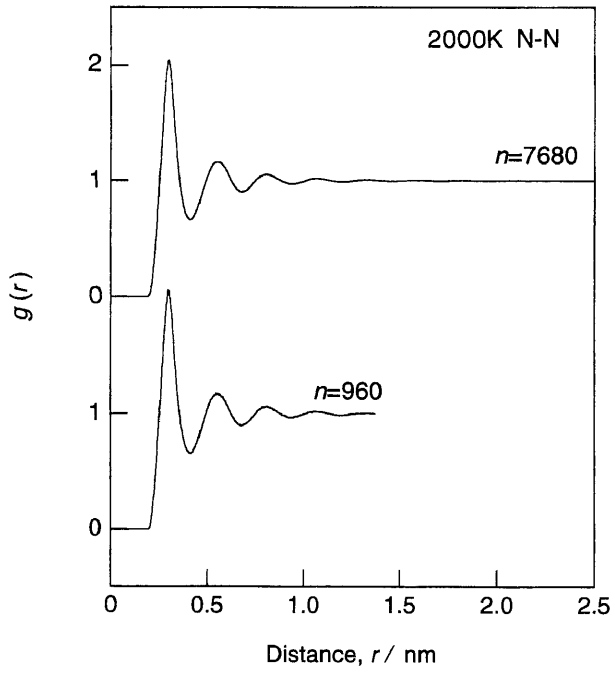

Fig. 1. Particle number terms of the pair distribution function at 2000 K for 960 and 7680 atom systems.

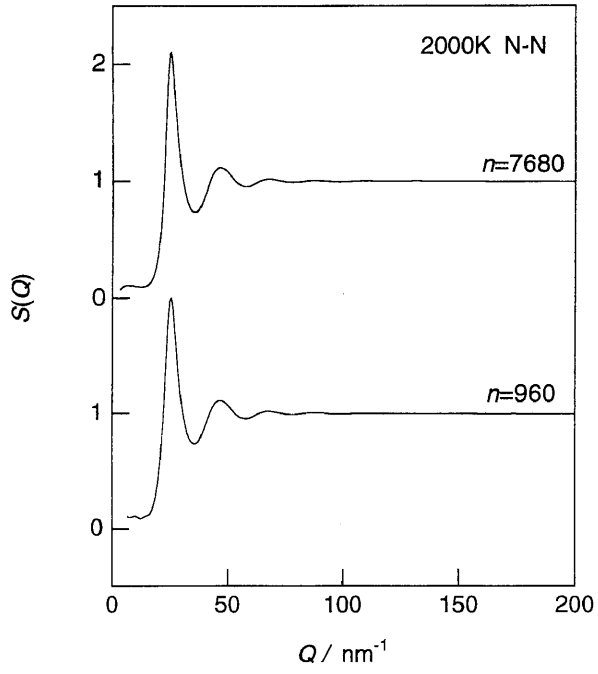

Fig. 2. Particle number terms of the structure factor at 2000 K for 960 and 7680 atom systems.

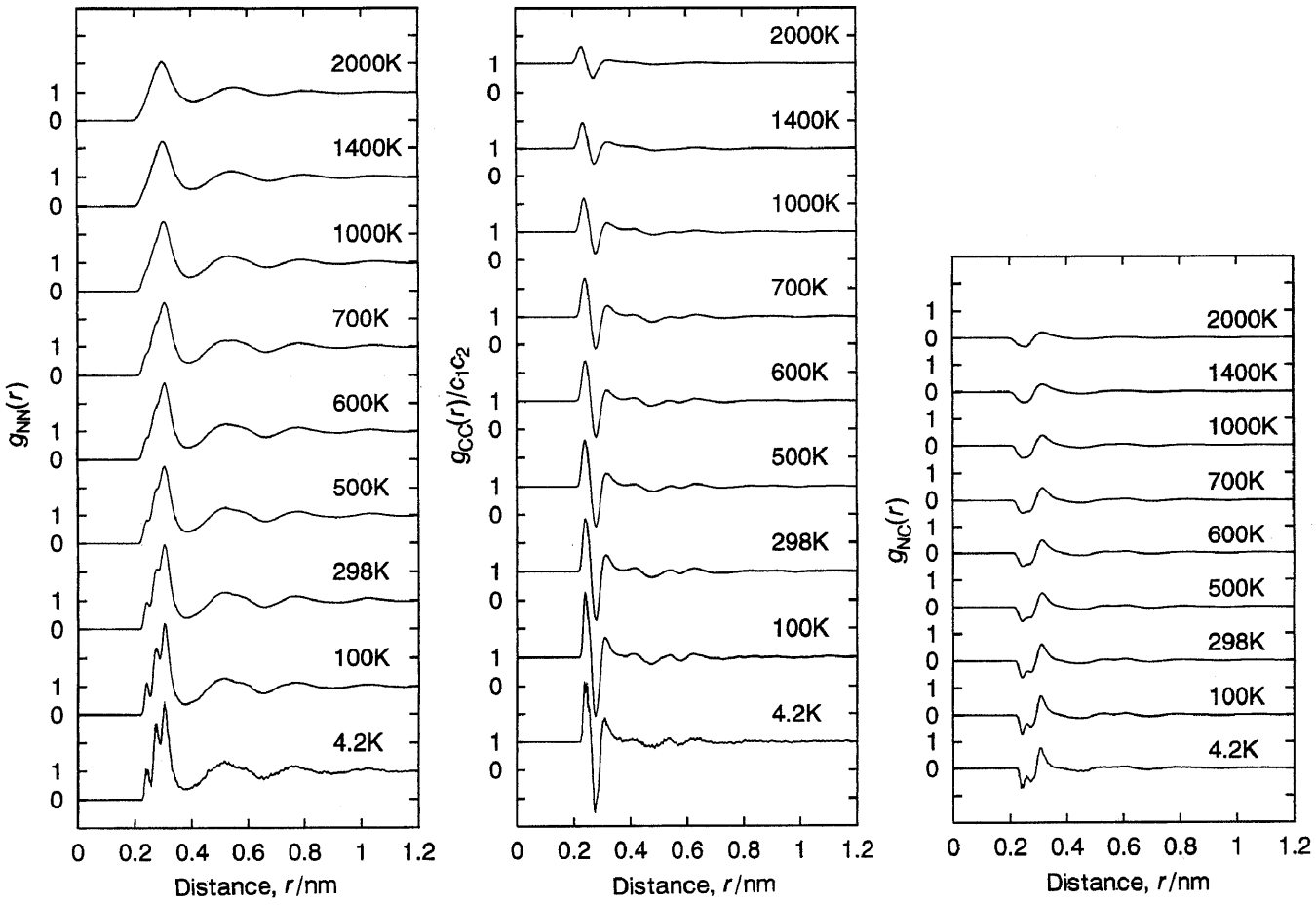

Fig. 3. Batia-Thornton type pair distribution functions, the particle number term, N-N, the concentration term, C-C, and their cross term, N-C.

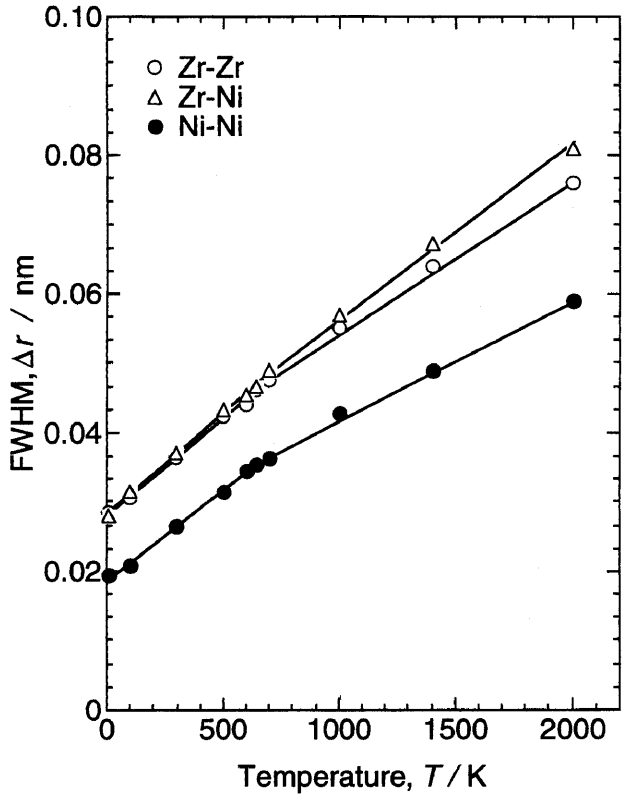

Fig. 4. Full width at half maximum (FWHM) of the first peaks of the Faber-Ziman type pair distribution function for Zr-Zr. Zr-Ni and Ni-Ni pairs.

VACF changes with temperature. Below the glass transition temperature, the VACF profile is almost the same at 640 and 298 K. Figure 6 shows the VACFs of Zr and Ni atoms at 500 K. The attenuation of the oscillation after first backscattering for the Zr atom is slower than that for the Ni atom. The atomistic dynamical behavior does not equivalent for all atomic species.

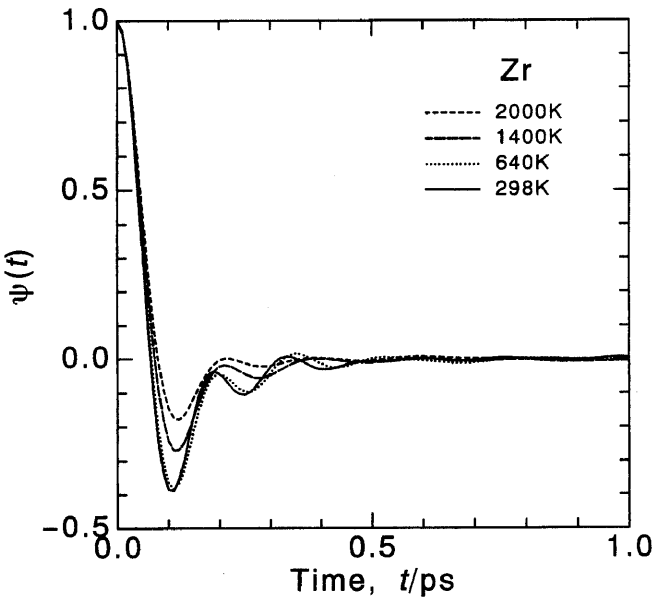

Fig. 5. Normalized velocity autocorrelation functions for Zr atom at various temperatures.

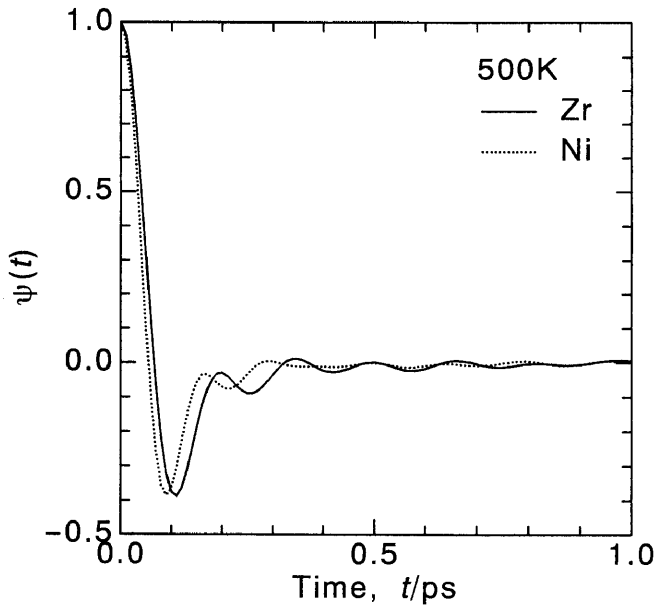

Fig. 6. Normalized velocity autocorrelation function for Zr and Ni atom at 500 K.

The normalized power spectra of the VACFs of Zr and Ni atoms are shown in Fig. 7. The angular frequency is indicated as the energy, the product of the frequency and Planck constant. The upper limits of the energy at 298 K is 35 meV for Zr and 43 meV for Ni. The frequency difference is caused by the atomic weight and potential difference. Below the glass transition temperature, $Z(0)$ is order of zero. It takes finite value for supercooled and equilibrium liquid states. For equilibrium state, the upper limit of the energy increases. Figure 8 shows the self [10] and mutual diffusion coefficients. The formar is calculated by Einstein formula and the latter is calculated by Green-Kubo formula. The self diffusion coefficient is guided by the Vogel-Fulcher relation rather than the Arrhenius relation. The lighter atom, Ni, diffuses faster than Zr. Since the Einstein formula is not satisfied below the glass transition temperature, the self diffusion coefficient is overestimated. [10] The mutual diffusion coefficient is less than the self diffusion coefficient over 1000 K and has the exponential temperature dependence.

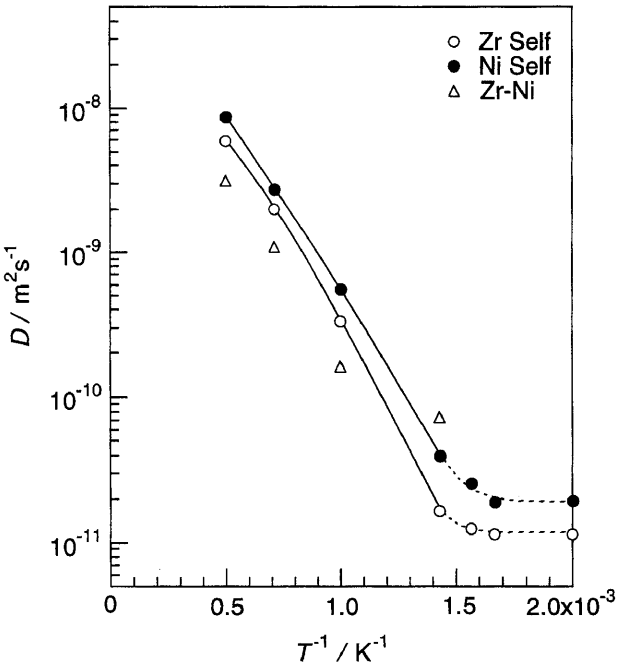

Fig. 8. Temperature dependences of diffusion coefficient for Zr, Ni and Zr-Ni.

The mutual diffusion coefficient is a collective quantity. As the dynamic quantity $j_{AB}(t)$ is already accumulated over all atoms, the ensemble average can not be performed for mutual diffusion. Then, simulation results for mutual diffusion are less precise than those for self diffusion obtained from simulation runs of the same time steps. [21] This problem is discussed in section 4.

3.3. Time dependent structure

The collective dynamics is a function of structure and motion. This is experimentally detected by neutron inelastic scattering. [10] We calculate the intermediate scattering function, [19] which is the time course of the density correlation in reciprocal space. The time variations of the coherent particle number term of the intermediate scattering functions are shown in Fig.9. The intermediate scattering function at $t = 0$ is equivalent to the structure factor. The first peak represents

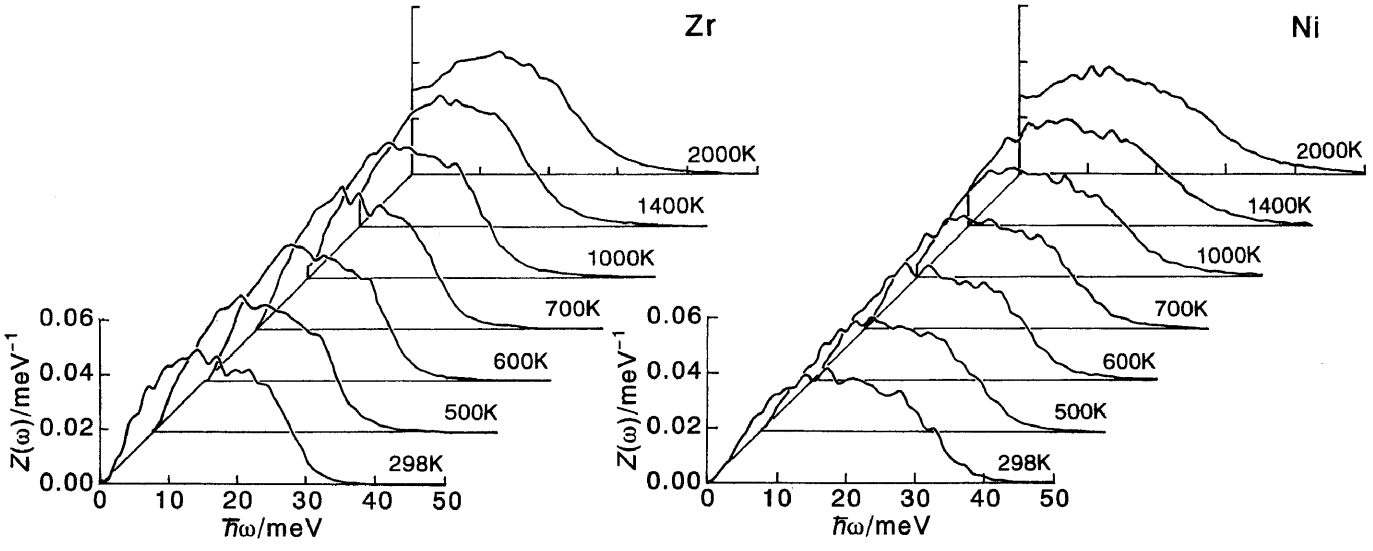

Fig. 7. Normalized power spectra of the velocity autocorrelation functions for Zr and Ni atoms at various temperatures.

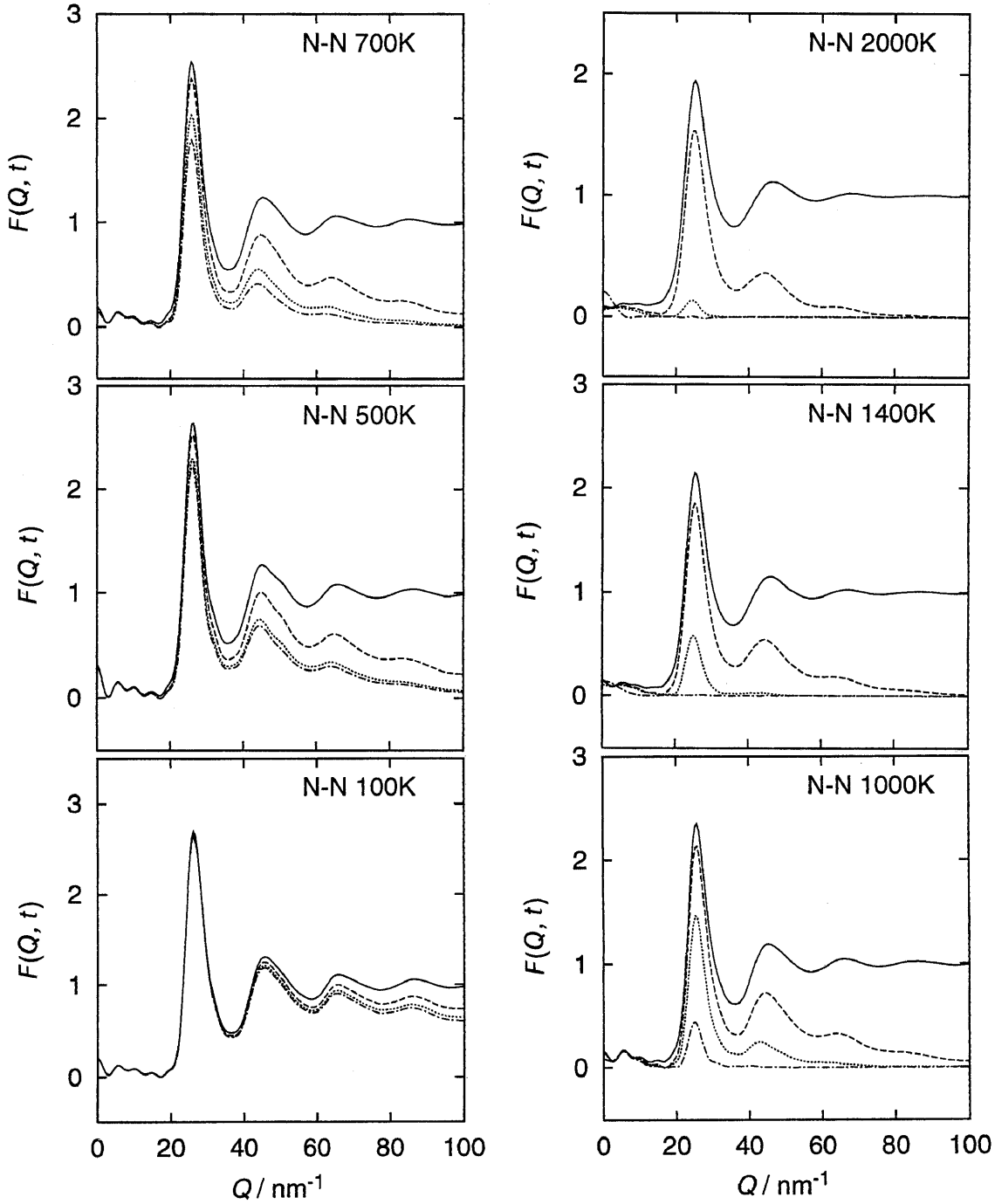

Fig. 9. Coherent particle number terms of intermediate scattering function at 0 ps (solid line), 0.1 ps (broken line), 1 ps (dotted line) and 10 ps (dashed and dotted line).

the correlation in an order of the first neighbor atom distance. The information at higher wave number is related to the fine shape of the pair distribution function. In the amorphous state at 100 K, the height of the first peak is almost constant. The atom does not move further than the nearest neighbor atom distance. The entire profile is almost fixed after 1 ps. The main motion is the thermal vibration and the relaxation for long time is rare. In the amorphous state at 500 K, the rate of variation for peak height is faster than that at 100 K. The fourth peak is almost disappeared after 10 ps. At 700 K, which is slightly higher than the glass transition temperature (640 K), the short time behavior is similar to that at 500 K. However, the change in the 700 K profile after 10 ps is greater than that at 500 K. This is caused by the relaxation for long time. In the supercooled liquid state at 1000 K, the profile changes drastically. Only the first peak correlation exists after 10 ps. The profile at low wave number also changes with time. In the equilibrium liquid state at 1400 K, the intermediate scattering function shows no correlation after 10 ps because of the active hydrodynamic diffusion.

Since the calculation of the van Hove correlation function for all atoms is time consuming, to examine the detail progress of the intermediate scattering function, we calculated the incoherent part. The time variations of the incoherent intermediate scattering function for Ni atom are shown in Fig. 10 with a logarithmic time scale. These results are obtained at the wave number Q=25.8nm^{-1}, i.e. the first peak of the static structure factor. The slowing behavior is similar

to the neutron measurement results of $Ca_{0.4}K_{0.6}(NO_3)_{1.4}$ salt (CKN). [24,25] In the supercooled liquid (1000 and 700K) and the amorphous (500 and 100K) states, two step relaxation is observed. The second (slow) decay is α relaxation, which is related to the hydrodynamic diffusion of the atom. The first (fast) decay is related to β relaxation, which is related to the thermal vibration. The relaxation time of α relaxation shows strong temperature dependence, but not for β relaxation. In the equilibrium liquid states, at 2000 and 1400K, the relaxation time for α relaxation decreases and is similar to that of the β relaxation, and the overall relaxation occurs as one process in the equilibrium liquid state.

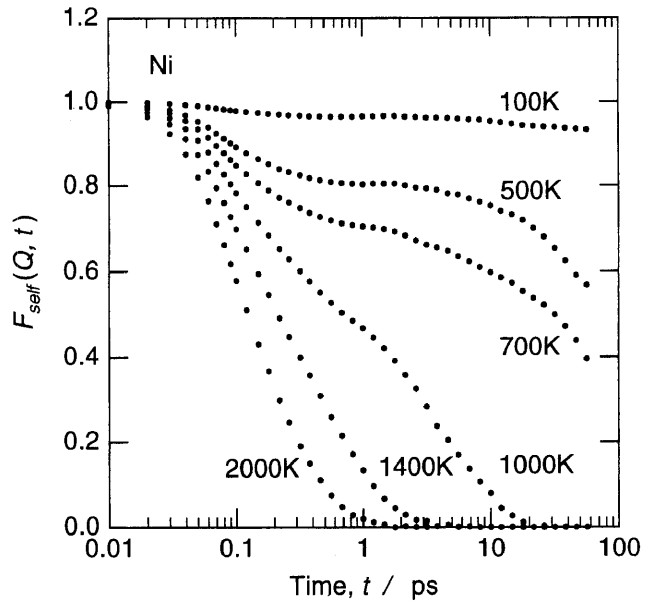

Fig. 10. Time variations of the incoherent intermediate scattering function of Ni atoms at various temperatures.

4. Discussion

The FWHM is a fluctuation from the averaged interatomic position. The origin of this fluctuation in amorphous and liquid states consists of three parts. The first is the fundamental static fluctuation caused by the non-periodicity. The second is the thermal vibration. The third is the hydrodynamic diffusion. The pair distribution function at very low temperature is mainly affected by the fundamental static fluctuation. At the high temperature in amorphous and liquid states, the thermal vibration is active. Over the glass transition temperature, the hydrodynamic diffusion occurs. The atoms frequently move from the first neighbor to the second neighbor position. This motion affects the shape of the first peak and the valley between the first and the second peak. The structural and the energetic properties obviously change through the glass transition temperature. On the other hand, the glass transition is not clearly detected by the dynamical properties derived from the present MD simulation. We observe the as quenched state in the MD simulation. In this case, the non-steady structural relaxations are frequently detected. Although the long time MD simulation over micro second is required to obtain the dynamic information under steady non-equilibrium state, such a large scale simulation can not be available even by the fastest super computer at present. This should be future problem.

The time correlation function $c(t)$ of the current $J(t)$ is

$$c(t)=\langle J(t)\cdot J(0)\rangle. \tag{15}$$

The integral of the time correlation function gives the transport coefficient K as

$$K=\int_0^\infty \langle J(t)\cdot J(0)\rangle dt. \tag{16}$$

This is the generalized form of Green-Kubo formula. This equation of statistical mechanics is defined for infinite size system and the integration is performed from zero to infinity. In MD analysis, however, we calculate the transport coefficient from finite data. If the correlation function converges to zero at finite time, it is a good approximation to replace infinite time by finite time in equation (16). The size effect for the accuracy depends on the current. The current is divided to three categories.

(a) In usual, the current is defined as the physical quantity $a(t)$ of one atom,

$$J(t)=a(t). \tag{17}$$

In this case, the ensemble average is available and the correlation function $c(t)$ is calculated with a good accuracy,

$$c(t)=\frac{1}{N}\sum_{j=1}^{N} a_j(t)\cdot a_j(0). \tag{18}$$

The velocity correlation function is an example.

(b) The current defined as a physical quantity with spatial correlation at wave vector Q is

$$J(Q,t)=\sum_{j=1}^{N} a_j(t)\exp\left(-iQr_j(t)\right). \tag{19}$$

The wave vector dependent correlation function is defined as

$$c(Q,t)=\langle J(Q,t)\cdot J(Q,0)\rangle. \tag{20}$$

If the spatial correlation length is smaller than the system size, i.e.,

$$|Q|>2\pi/L, \tag{21}$$

the correlation function is spatially averaged with relatively high accuracy. The particle current correlation function [8] and the dynamic structure factor calculations correspond to this case. [9]

(c) The current defined as a summation of the physical quantity of all the atoms is a special case of equation (19) with $Q\rightarrow 0$. The wave vector limit is replaced by the infinite number of atoms.

$$J(0,t)=\lim_{Q\rightarrow 0}\sum_{j=1}^{N} a_j(t)\exp\left(-iQr_j(t)\right)$$

$$\approx \lim_{N\to\infty} \sum_{j=1}^{N} a_j(t), \tag{22}$$

and

$$c(0,t) = \left\langle \lim_{Q\to 0} J(Q,t)\cdot J(Q,0) \right\rangle$$

$$\approx \lim_{N\to\infty} \left\{ \sum_{j=1}^{N} a_j(t) \right\} \cdot \left\{ \sum_{j=1}^{N} a_j(0) \right\}. \tag{23}$$

Because the number of the atoms in MD simulation is much smaller than infinity (at most ~ 10^6), the accuracy of the correlation function is rather low. The mutual diffusion coefficient and viscosity are such examples.

5. Summary

We have performed the molecular dynamics simulations for the amorphous and liquid $Zr_{67}Ni_{33}$ alloys with a pair functional potential. The size effect of MD system is examined for the structure of the equilibrium liquid state. The 960 atom system provides the same results as the 7680 atom system except for long range correlation.

The temperature dependence of the pair distribution function is studied. The feature changes sharper with decreasing temperature. The concentration fluctuation over the second neighbor atom is small for amorphous and liquid states. The full width at half maximum (FWHM) for the pair distribution function increases with temperature. Its temperature derivative changes at the glass transition temperature. The hydrodynamic diffusion affects this structural change through the glass transition.

The non collective single particle motion is analyzed by the velocity autocorrelation function (VACF) and its power spectra. Over the glass transition temperature, the behavior of the VACF changes with temperature. The upper limit of the energy of the power spectra of the VACF for Ni atom is higher than that for Zr atom. The mutual and self diffusion coefficients are calculated. The self diffusion coefficient shows Vogel-Fulcher type temperature dependence.

The collective dynamics is analyzed by the intermediate scattering function. The decrease of the coherent part intermediate scattering function at 10 ps is obviously observed above the glass transition temperature. This is caused by the long time relaxation. The detail of the time evolution of the incoherent part of intermediate scattering function is calculated at the wave number of the first peak of the static structure factor. The intermediate scattering function clearly reveals two relaxation processes, α and β, below the melting point. For the equilibrium liquid state, the relaxation times of the α and β relaxations are of the same order. Therefore, the relaxation is detected as one process.

The accuracy of the transport coefficient derived from Green-Kubo formula depends on the style of the current. For the current defined as the physical quantity of one atom, the ensemble average of the correlation function is available, and the transport coefficient is calculated with high accuracy.

Acknowledgments

The numerical calculations were performed by the supercomputing system HITAC S-3800/380 at Institute for Materials Research (IMR), Tohoku University. The authors are indebted to the Information Science Group of IMR, Tohoku University for their continuous support. The authors acknowledge gratefully partial support of this work by the Grant-in-Aid for Scientific Research on Priority Area of "Development of Micro-Heat Transfer for Manufacturing and Processing of New Materials." (No. 06230201) and the Grant-in-Aid for Encouragement of Young Scientists (No. 06855073).

1) G. Ciccotti, D. Frenkel, I. R. McDonald: *Simulation of liquids and solids* , (North-Holland, Amsterdam, 1990).
2) W. G. Hoover: *Molecular Dynamics.*, (Springer-Verlag, Berlin, 1986).
3) F. Yonezawa: Solid State Physics, **45** (1991) 179.
4) G. Wahnstrom: Phys. Rev., **A44** (1991) 3752.
5) G. Wahnstrom: J. Non-Cryst. Solids, **A131-133** (1991) 109.
6) T. Aihara Jr., K. Aoki, T. Masumoto: Scr. Metall., **28** (1993) 1003.
7) T. Aihara Jr., K. Aoki, T. Masumoto: Mater. Sci. Eng., **A179-180** (1994) 256.
8) T. Aihara Jr., T. Masumoto: J. Phys. Condensed Matter, **7** (1995) 1525.
9) T. Aihara Jr., K. Aoki, T. Masumoto: Mater. Trans. JIM, **36** (1995) in press.
10) T. Aihara Jr., T. Masumoto: Mater. Trans. JIM, to be published.
11) Z. Altounian, T. Guo-hua, J. O. Strom-Olsen: J. Appl. Phys., **54** (1983) 3111.
12) M. P. Henaff, C. Colinet, A. Pasturel, K. H. J. Buschow: J. Appl. Phys., **56** (1984) 307.
13) A. Lee, G. Etherington, C. N. J. Wagner: J. Non-Cryst. Solids, **61&62** (1984) 349.
14) J. B. Suck: in *Dynamics of disordered materials,* D. Richter, A. J. Dianoux, W. Petry, J. Teixeria, Eds. (Springer-Verlag, Berlin, 1989), p. 182.
15) S. Nosè: J. Chem. Phys., **81** (1984) 511.
16) Z. Altounian, J. O. Strom-Olsen: Phys. Rev., **B27** (1983) 4149.
17) T. B. Massalsky, Ed.: *Binary alloy phase diagrams, 2nd Ed.* (ASM international, Materials park, OH, 1991).
18) C. Massobrio, V. Pontikis, G. Martin: Phys. Rev., **B41** (1991) 10486.
19) J. P. Hansen, I. R. McDonald: *Theory of simple liquids, 2nd Ed.* (Academic Press, London, 1986).
20) Y. Waseda: *The structure of non-crystalline materials.* (McGraw-Hill, New York, 1980).
21) J. M. Hail: *Molecular dynamics simulation.* (John Wiley & Sons, New York, 1992).
22) H. R. Wendt, F. F. Abraham: Phys. Rev. Lett., **41** (1978) 1244.
23) K. Suzuki: in *Neutron scattering (Method of experimental physics, Part B),* K. Skold, D. L. Price, Eds. (Academic Press, London, 1987), vol. 23, p. 243.
24) W. Knaak, F. Mezei, B. Farago: Europhys. Lett., **7** (1988) 529.
25) F. Mezei, W. Knaak, B. Farago: Phys. Rev. Lett., **58** (1987) 571.